Hyperlipidemia offers protection against *Leishmania donovani* infection: role of membrane cholesterol[s]

June Ghosh,* Shantanabha Das,* Rajan Guha,* Debopam Ghosh,[1],* Kshudiram Naskar,* Anjan Das,[†] and Syamal Roy[2],*

*Department of Infectious Diseases and Immunology, Indian Institute of Chemical Biology, Jadavpur, Kolkata-700032, India; and [†]Department of Pathology, Calcutta National Medical College and Hospital, Beniapukur, Kolkata-700014, India

Abstract *Leishmania donovani* (LD), the causative agent of visceral leishmaniasis (VL), extracts membrane cholesterol from macrophages and disrupts lipid rafts, leading to their inability to stimulate T cells. Restoration of membrane cholesterol by liposomal delivery corrects the above defects and offers protection in infected hamsters. To reinforce further the protective role of cholesterol in VL, mice were either provided a high-cholesterol (atherogenic) diet or underwent statin treatment. Subsequent LD infection showed that an atherogenic diet is associated with protection, whereas hypocholesterolemia due to statin treatment confers susceptibility to the infection. This observation was validated in apolipoprotein E knockout mice (AE) mice that displayed intrinsic hypercholesterolemia with hepatic granuloma, production of host-protective cytokines, and expansion of anti-leishmanial CD8$^+$IFN-γ^+ and CD8$^+$IFN-γ^+TNF-α^+ T cells in contrast to the wild-type C57BL/6 (BL/6) mice when infected with LD. Normal macrophages from AE mice (N-AE-Mϕ) showed 3-fold higher membrane cholesterol coupled with increased fluorescence anisotropy (FA) compared with wild-type macrophage (N-BL/6-Mϕ). Characterization of in vitro LD-infected AE macrophage (LD-AE-Mϕ) revealed intact raft architecture and ability to stimulate T cells, which were compromised in LD-BL/6-Mϕ.[SD] This study clearly indicates that hypercholesterolemia, induced intrinsically or extrinsically, can control the pathogenesis of VL by modulating immune repertoire in favor of the host.—Ghosh, J., S. Das, R. Guha, D. Ghosh, K. Naskar, A. Das, and S. Roy. Hyperlipidemia offers protection against *Leishmania donovani* infection: role of membrane cholesterol. *J. Lipid Res.* 2012. 53: 2560–2572.

Supplementary key words apolipoprotein E • hypercholesterolemia • membrane fluidity • CD8$^+$ T cells

Visceral leishmaniasis (VL) or kala-azar is characterized by the inability of the host to develop antileishmanial immune response (1–3). *Leishmania donovani* (LD), during their intracellular life cycle within macrophage cells (4, 5), extract membrane cholesterol (6), and its replenishment via liposomal cholesterol offers protection in LD-infected hamsters (7). VL patients show reduced serum cholesterol as a function of splenic parasite load (8, 9).

Hypocholesterolemia is a prognostic indicator of increased morbidity and mortality connected with pathological conditions (10, 11). Hypocholesterolemic men show lower total T cells, fewer CD8$^+$ and CD4$^+$ T cells, and a lower production of interleukin (IL)-2 than hypercholesterolemic men (10). There is a report that *M. tuberculosis* metabolizes cholesterol, which is crucial for bacterial persistence (12). Cholesterol therapy is in clinical use either alone or in combination with drugs. Oral administration of cholesterol shows profound improvement in pulmonary tuberculosis and Smith-Lemli-Opitz syndrome (13).

Cholesterol plays an important role in the maintenance of membrane fluidity essential for proper antigen-presenting cell (APC) function (14). Cholesterol is also essential for formation of membrane rafts, (15, 16) which are important pathogen portals (17–20) required for *Leishmania* entry (21). It also promotes phagocytosis of *Helicobacter pylori* by APCs and influences generation of antigen-specific T-cell response (22).

Abbreviations: AE, apolipoprotein E knockout mice; APC, antigen-presenting cell; BL/6, C57BL/6 mice; CTX-B, cholera toxin B subunit; FA, fluorescence anisotropy; IL, interleukin; INF, interferon; LD, *Leishmania donovani*; LD-AE, *Leishmania donovani*-infected apolipoprotein E knockout mice; LD-AE-Mϕ, *Leishmania donovani*-infected apolipoprotein E knockout macrophage; LD-BL/6, *Leishmania donovani*-infected C57BL/6 mice; LD-BL/6-Mϕ, *Leishmania donovani*-infected C57BL/6 macrophage; N-AE-Mϕ, normal apolipoprotein E knockout macrophage; N-BL/6-Mϕ, normal C57BL/6 macrophage; PEC, peritoneal exudate cell; SLA, soluble leishmanial antigen; TGF, Transforming growth factor; TNF, tumor necrosis factor; VL, visceral leishmaniasis.

[1] Current address for D.G.: Interdisciplinary Biomedical Science, University of Arkansas for Medical Science, Little Rock, AR 72205.

[2] To whom correspondence should be addressed.
  e-mail: sroy@iicb.res.in

[s] The online version of this article (available at http://www.jlr.org) contains supplementary data in the form of three figures and one table.

Genetic mutants of sterol metabolism show an altered lipid profile as evident from studies on low-density lipoprotein receptor (LDLR) knockout and apolipoprotein E knockout mice strains (23). Apolipoprotein (apo)E, a 34 kDa glycoprotein synthesized mainly in the liver and brain, is a constituent of all lipoproteins except low-density lipoproteins (LDL) (24). Human apoE is polymorphic with three isoforms: apoE2, apoE3, and apoE4, of which apoE2 is associated with genetic hyperlipoproteinemia type III. In rodents, however, there is only one isoform of apoE. ApoE exerts its biological functions, including clearance of chylomicrons and very low density lipoprotein (VLDL) remnants by binding to its receptors, the LDLR family (25).

Serum lipoproteins may contribute to the host innate immunity against pathogen attack. ApoE knockout (AE) mice were reported to have impaired defense against *Listeria monocytogenes* and *Klebsiella pneumonia* infections (26, 27). In contrast, AE mice showed protection against tuberculosis (28) and reduced production of infectious hepatitis C virus (HCV) (29).

In the present study, we demonstrate that hypercholesterolemia, either by genetic manipulation or induced diet, leads to protection against *Leishmania donovani* infection. In contrast, statin treatment both in AE and BL/6 mice leads to hypocholesterolemia, rendering the mice susceptible to the parasite infection. Interestingly, BALB/c mice known to be susceptible to LD infection can also be protected by a high-cholesterol diet.

MATERIALS AND METHODS

Reagents and antibodies

RPMI-1640 and M-199 medium, HBSS buffer, sodium bicarbonate,1,6-diphenyl-1,3,5-hexatriene (DPH), Giemsa stain, 2-ME, FITC-conjugated cholera toxin B subunit (CTX-B-FITC), ConA, Ionomycin, PMA, Ovalbumin, RBC lysis buffer, TMB, and hematoxylin and eosin were purchased from Sigma-Aldrich. Fetal calf serum (FCS) and penicillin-streptomycin mixture were obtained from GIBCO. Amplex Red kit and Fluo-4-AM were purchased from Molecular Probes (Invitrogen). Tetrahydrofuran was purchased from Qualigens. Trizol, LIVE/DEAD Fixable Aqua Dead Cell stain kit and Reverse Transcription kit were obtained from Invitrogen. SYBR green mix was purchased from Applied Biosystems. Biotinylated anti-mouse CD71, biotinylated anti-mouse I-A^b, and streptavidin-FITC were purchased from BD Biosciences. Paraformaldehyde was purchased from USB Biochemicals. VECTASHIELD Mounting Medium with DAPI was obtained from Vector Laboratories. ELISA kits for IL-2, IL-4, IL-6, IL-10, IL-12, tumor necrosis factor (TNF)-α, transforming growth factor (TGF)-β, and interferon (IFN)-γ were purchased from BD Biosciences, while IL-17 and IL-22 were purchased from R and D Systems. Brefeldin, FcR blocking reagent, anti-mouse CD3 PE-Cy7, anti-mouse CD4 PerCP, anti-mouse CD8 APC-Cy7, anti-mouse TNF-α FITC, and permeabilization and fixation kit were purchased from BD Biosciences. Anti-mouse IFN-γ Pacific Blue was procured from BioLegend. Atorvastatin (Atorva 20) was purchased from Zydus Medica. Atherogenic rodent diet (1.25% cholesterol) was from Harlan Laboratories.

Cell line

MHC class II (I-A^b)-restricted Ova-specific T-cell hybridoma 13.8 (30) was a kind gift from Dr. Satyajit Roth (National Institute of Immunology, New Delhi, India). It was maintained in RPMI 1640 medium supplemented with 10% FCS and 2-ME at 37°C with 5% CO_2 in a humidified atmosphere.

Ethics statement

Use of mice was approved by the Institutional Animal Ethics Committee of the Indian Institute of Chemical Biology, India. All the experiments were performed according to the National Regulatory Guidelines issued by the Committee for the Purpose of Supervision of Experiments on Animals, Ministry of Environment and Forest, Government of India. All experiments involving animals were carried out with prior approval of the institutional animal ethics committee.

Animals and treatments

Four-week-old BALB/c, C57BL/6 (hereafter called BL/6), and apoE knockout (hereafter called AE) mice were brought from the Central Drug Research Institute, India, animal facility (originally from the Jackson Laboratory). AE mice were obtained by insertion of a neomycin resistance cassette that deleted part of exon 3 and part of intron 3 of the *apoe* gene (http://jaxmice.jax.org/strain/007069.html). They were kept under conventional conditions with food (standard rat chow diet) and water provided ad libitum. For statin treatment, atorvastatin was orally given at a dose of 50 mg/kg body weight/day for three weeks before infection was delivered (31). Animals fed a high-cholesterol diet were given the atherogenic diet (28) for the whole period of the experiment. In all experiments, six animals were kept in each group.

Parasites, infection, and preparation of SLA

L. donovani strain AG83 (MAOM/IN/1083/AG83), originally obtained from an Indian kala-azar patient, is maintained in golden hamsters (32). As and when needed, the infected animals were euthanized, and amastigotes that were isolated from spleen were transformed to promastigotes. Statin-treated, chow and atherogenic diet fed BALB/c, BL/6, and AE mice were inoculated with 10 million second/third passage promastigotes via intracardiac injection (32). Soluble leishmanial antigen (SLA) was prepared after repeated freeze-thaw cycles and sonication of promastigotes as described previously (33).

Diets

Two diets were used: *i*) a normal chow diet that contained 4% (wt/wt) animal fat and <0.04% (wt/wt) cholesterol, and *ii*) a 1.25% cholesterol/ atherogenic diet (TD.02028 from Harlan Laboratories). The final diet contained 1.25% cholesterol, 5% (wt/wt) cellulose, 19.5% casein, and 0.5% (wt/wt) cholic acid.

Estimation of serum lipid profile

Animals were anesthetized, and blood was collected from heart before euthanasia. Blood was kept at rest at 4°C, and separated serum was isolated. This serum was stored at −80°C. Eventually the lipid profile was estimated in a certified pathological laboratory using lipid estimation kits from Merck using the enzymatic method for cholesterol, triglyceride, and HDL and the direct method for LDL. VLDL was determined using standard calculations.

Determination of parasite load

Splenic and hepatic parasite burdens were determined by the impression smear method as described (34). The results are expressed as the number of parasites per spleen or per liver, respectively.

Histology

For hepatic tissue response in mice, liver sections from six-week-infected BL/6 and AE mice were assessed microscopically after staining with hematoxylin and eosin as previously described (35). Briefly, portions of liver tissue were first fixed in 10% formalin, and tissue sections were stained after standard processing (e.g., paraffin embedding, histological sectioning, and mounting on glass slides). Sections from each liver were examined under a ×400 magnification light microscope.

Isolation of spleen cells and in vitro restimulation

Spleens, aseptically removed from euthanized animals, were passed through sterile 100 μm cell strainers to prepare single-cell suspension. To remove red blood cells, splenocytes were treated with RBC lysis buffer (Sigma-Aldrich) and later washed with complete cell culture media. Cells were seeded in tissue culture plates in complete media alone or with SLA (50 μg/ml) and ConA (5 μg/ml), and then incubated for 72 h (36). Restimulation assays were done in triplicate for each condition. Supernatants and cells were harvested for subsequent analyses.

Cytokine assay

Culture supernatants from in vitro-stimulated splenocyte cultures were used to assay IL-2, IL-4, IL-6, IL-10, IL-12, IL-17, IL-22, TNF-α, TGF-β, and IFN-γ using ELISA according to the manufacture's protocol. TGF-β was measured as described (37). Briefly, culture supernatants were acidified to activate the latent TGF-β by adding 1 N HCl to cell supernatant at a 1:1 ratio for 10 min and neutralizing with 1.2 N NaOH. These processed samples were subsequently used for assay.

Flow cytometric analysis of intracellular cytokines

Sample preparation for flow cytometric analysis of intracellular cytokine staining was performed as previously described (38, 39) with slight modifications. Briefly, cells cultured for 72 h with 50 μg/ml of SLA stimulation were harvested and restimulated with 5 ng/ml PMA and 0.5 μg/ml ionomycin for 6 h, the last 4 h in the presence of Brefeldin (10 μg/ml). Cells were at first blocked with Fc receptor blocker for 10 min at 4°C. Initially, anti-mouse CD3, anti-mouse CD4, anti-mouse CD8, and LIVE/DEAD Aqua were used to stain surface markers. Then cells were washed, fixed, and permeabilized with BD fix/perm reagent. Cells were washed again, and anti-mouse IFN-γ and anti-mouse TNF-α antibody was added to stain intracellular cytokines. Cells were washed again, and samples were acquired on BD FACSAria- II flow cytometer (BD Biosciences). All flow cytometry data were analyzed with FlowJo Software (Tri star Inc.).

Real-time quantitative RT-PCR

Total RNA was extracted with Trizol reagent from 3×10^6 splenocytes, according to the manufacturer's (Invitrogen) instructions. The precipitated RNA pellet was washed in 80% ethanol, air dried, and dissolved in nuclease free water. RNA concentration was determined using a nanodrop spectrophotometer.

mRNA of T-bet, GATA3, ROR-γt quantification was done using standard SYBR green real-time PCR assays (Applied Biosystems). The primer sequences are as follows: T-bet forward, 5′-CCCACAAGCCATTACAGGATG-3′; reverse, 5′-TATAAGCG-GTTCCCTGGCATG-3′; GATA3 forward, 5′-AGGAGTCTCCA-AGTGTGCGAA-3′; reverse, 5′-TTGGAATGCAGACACCACCT-3′; ROR-γt forward, 5′-TGGAAGATGTGGACTTCGTTT-3′; reverse, 5′-TGGTTCCCCAAGTTCAGGAT-3′; β-actin forward, 5′AGCTGC-GTTTTACACCCTTT-3′ reverse, 5′-AAGCCATGCCAATGTTG-TCT-3′.

The reverse transcription reaction was carried out with random hexamer, 1.0 μg of total RNA, and the M-MLV RT enzyme from Invitrogen according to manufacturer`s protocol. cDNA was subsequently diluted twice in nuclease-free water before addition to the RT-PCR reaction mixture. The Applied Biosystems 7500 real-time PCR instrument was used for amplification. The results were normalized against β-actin. Data points are relative fold changes (R_q) with respect to normal BL/6 values. Basically, $2^{-\Delta Ct}$ [where ΔCt = Threshold cycle (Ct) target − Threshold cycle of endogenous control (here, β-actin)] values were calculated for each group from three different experiments; means were determined and represented as fold changes taking normal BL/6 to be 1.

Isolation of peritoneal exudate cells and in vitro infection

Elicited peritoneal exudate cells (PEC) were isolated as described previously (40) and kept in tissue culture plates for 48 h. PECs were either kept untreated or infected with *L. donovani* promastigotes in the ratio of 1:10 PEC:parasite. Six hours after addition, excess parasites were washed out, and cells were kept for 48 h in complete media. For convenience, PEC were defined as macrophages or antigen-presenting cells (APC) interchangeably. Macrophages from normal BL/6 mice and normal AE mice were defined as N-BL/6-Mφ and N-AE-Mφ, respectively. Similarly, in vitro LD-infected macrophages from BL/6 and AE mice were defined as LD-BL/6-Mφ and LD-AE-Mφ, respectively.

Quantification of membrane cholesterol with an Amplex Red assay kit

The macrophage membrane was prepared as described previously (41) with some modifications. Briefly, macrophages underwent repeated freezing and thawing cycles, and cells were partially ruptured by syringe-passing procedures. The homogenate was centrifuged at 900 *g* for 10 min at 4°C. The supernatant was filtered through nylon mesh (100 μm), and the pellet was discarded. The supernatant was further centrifuged at 50,000 *g* for 20 min at 4°C. The resulting pellet was suspended in buffer containing 50 mM Tris, 1 mM EDTA, 0.24 mM PMSF, 10 mM iodo-acetamide (pH 7.4) and centrifuged again at 100,000 *g* for 20 min at 4°C. The final pellet (native membranes) was suspended in a minimum volume of buffer containing 50 mM Tris (pH 7.4), flash-frozen in liquid nitrogen, and stored at −70°C. The protein content of the membrane was determined using Bio-Rad reagent according to the manufacturer's protocol. The total cholesterol content, both esterified and free, was determined by using an Amplex Red reagent kit (42), and the results were expressed in μmol cholesterol/μg protein.

Measurement of fluorescence anisotropy

The membrane fluorescence and lipid fluidity of cells were measured as per the method described (43). Briefly, the fluorescent probe DPH was dissolved in tetrahydrofuran at 2 mM concentration. Then 10^6 cells were mixed with an equal volume of DPH in PBS (C_f 1 μM) and incubated for 2 h at 37°C for labeling the cell membrane. Thereafter, the cells were washed twice and resuspended in PBS. The DPH probe bound to the membrane of the cell was excited at 365 nm, and the intensity of emission was recorded at 430 nm in a spectrofluorometer. The fluorescence anisotropy (FA) value was calculated using the equation: FA = $[(I_\parallel - I\perp)/(I_\parallel + 2I\perp)]$, where $I_\parallel$ and $I_\perp$ are the fluorescent intensities oriented, respectively, parallel and perpendicular to the direction of polarization of the excited light (44).

Confocal microscopy

All macrophages (N-BL/6-Mφ, N-AE-Mφ, LD-BL/6-Mφ, and LD-AE-Mφ) were stained with fluorochrome-conjugated Ab

according to the manufacturer's protocol. Briefly, FITC-conjugated CTX-B or biotin-conjugated-anti CD71 was diluted to a predetermined optimal concentration in 50 µl of FACS buffer. Cover slips were inverted upside down over the diluted conjugate to form a uniform monolayer and incubated at 4°C for 30 min in the dark. The reaction was stopped by adding 200 µl of FACS buffer and washing three times. For CD71 staining, FITC-conjugated streptavidin staining was done in a similar manner. The cells were then fixed with 1% paraformaldehyde, mounted with VECTASHIELD-DAPI on a glass slide, and observed under a laser scanning confocal microscope (NIKON, A1R, JAPAN) using 60× oil for magnification and 404 nm and 488 nm laser for all studies. The software used for image analysis is NIS-Elements Viewer.

Antigen presentation assay and quantitative I-A^b expression

Either normal or 48 h infected macrophages were incubated with anti-Ova T-cell hybridoma 13.8, with or without ovalbumin for 16–20 h at a fixed ratio of 1:10 APC:T cell in complete RPMI 1640 medium. The culture supernatants were analyzed for the presence of IL-2 by ELISA. To study the expression of I-A^b, macrophage cells were stained with FITC-conjugated anti-I-A^b and analyzed for expression of I-A^b by flow cytometry. The results were expressed as mean fluorescence intensity values.

Intracellular calcium mobilization

Intracellular calcium mobilization in anti-Ova T-cell hybridoma 13.8 in response to ova-pulsed and unpulsed APCs was measured fluorometrically. T cells (13.8) were loaded with calcium-sensing Fluo-4-AM at a final concentration of 4 µM (45), washed with calcium-free HBSS buffer, and resuspended in HBSS buffer containing 0.5 µM EGTA at a concentration of 10^6 cells/ml. The suspension (1 ml) was placed in a continuously stirred cuvette at 37°C in a fluorimeter. After ~1 min of scanning, appropriate antigen pulsed and unpulsed APCs were added to the cuvette, and fluorescence was monitored in real time at $Ex_{max} = 494$ nm and $Em_{max} = 516$ nm.

Statistical analysis

All experiments were done three times; inter-assay variation was within 5–10%. Data points are mean ± SEM or mean ± SD. All graphs and statistical analyses were generated in GraphPad Prism 5.00 (GraphPad, San Diego, CA). Nonparametric unpaired t-test

was used for analysis. We considered P less than 0.05 statistically significant. P less than 0.001 was considered extremely significant (***); P between 0.001 and 0.01 was considered very significant (**); P between 0.01 and 0.05 was considered significant (*); and P greater than 0.05 was considered not significant (ns).

RESULTS

ApoE knockout mice show significantly lower organ parasite burden compared with wild-type mice

ApoE knockout mice (AE) and its wild-type counterpart C57BL/6 mice (BL/6) were infected with LD, and splenic and hepatic parasite burdens were determined in a longitudinal infection. At three weeks postinfection, there was slightly lower splenic parasite load in infected AE (LD-AE) mice compared with infected BL/6 (LD-BL/6) mice ($P < 0.01$). At six weeks postinfection, the splenic parasite load continued to increase in wild-type, whereas the same decreased dramatically in LD-AE mice ($P < 0.0001$) (**Fig. 1A**). The picture was somewhat different in liver. At three weeks postinfection, there was comparable hepatic parasite burden in both mice strains. Interestingly, at six weeks postinfection, there was a drastic decrease in hepatic parasite burden in LD-AE animals, whereas it increased further in the wild-type counterpart ($P < 0.0001$) (Fig. 1B).

Atherogenic diet decreases and statin treatment increases organ parasite load

To show that cholesterol status indeed has a significant bearing on the pathogenesis of LD infection; BALB/c, BL/6, and AE mice were fed normal chow diet or high-cholesterol atherogenic diet or treated with atorvastatin. From the lipid profile (supplementary Table I), it was apparent that statin treatment decreased the serum cholesterol (around 40%, 33%, and 50% reduction in BL/6, AE, and BALB/c, respectively), whereas atherogenic diet induced hypercholesterolemia (around 2-, 4-, and 1.7-fold increase in BL/6, AE, and BALB/c, respectively). Triglyceride
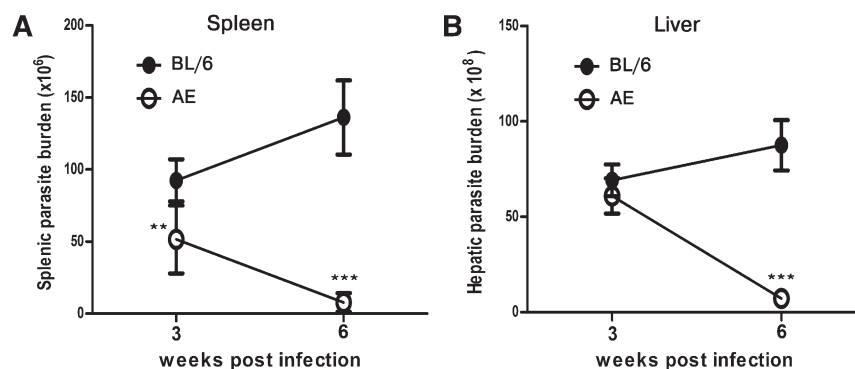

Fig. 1. Organ parasite burden in LD-BL/6 and LD-AE mice. Six-week-old mice were infected intracardially with 10^7 stationary-phase promastigotes. The animals were euthanized at indicated intervals, and the organ parasite burden was estimated by impression smear method using Geimsa stain. (A) Splenic parasite burden at three weeks and six weeks postinfection, respectively. (B) Hepatic parasite burden at three weeks and six weeks postinfection, respectively. n = 6 for each group. The data represents mean ± SEM from three different experiments. ***$P < 0.001$, **$0.001 < P < 0.01$, *$0.01 < P < 0.05$.
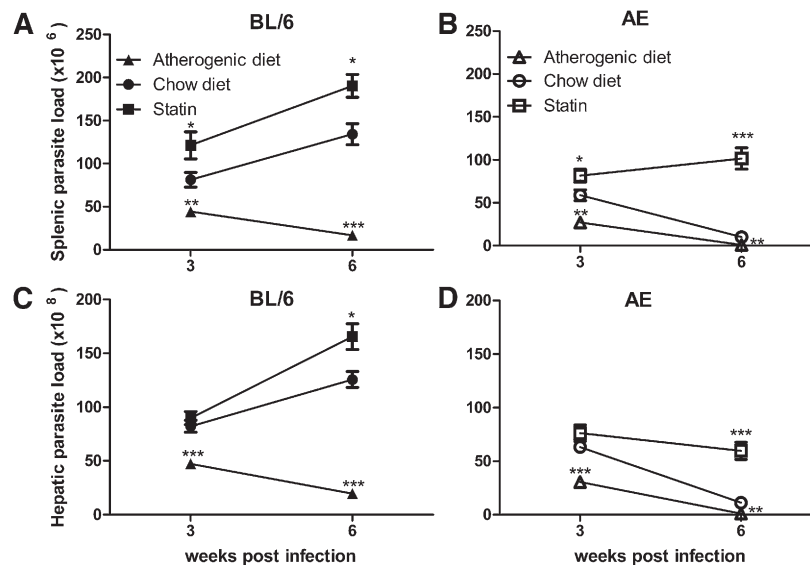
Fig. 2. Organ parasite burden in infected BL/6 and AE mice on variable treatments. Four-week-old mice were either treated with atorvastatin (50 mg/kg body weight per day) or fed a high-cholesterol atherogenic diet. After three weeks posttreatment, all animals were challenged with 10^7 stationary-phase promastigotes via the cardiac route. Statin injection was discontinued while the atherogenic diet was continued until the termination of the experiment at six weeks postinfection. Control and statin-treated groups received standard rat chow diet during the whole experiment. The animals were euthanized at indicated intervals, and organ parasite burden was estimated by impression smear method using Geimsa stain. (A) Splenic parasite burden in LD-BL/6 mice. (B) Splenic parasite burden in LD-AE mice. (C) Hepatic parasite burden in LD-BL/6 mice. (D) Hepatic parasite burden in LD-AE mice. n = 6 for control and atherogenic diet groups, and n = 4 for statin-treated group. The data represents mean ± SEM from two different experiments. ***$P < 0.001$, **$0.001 < P < 0.01$, *$0.01 < P < 0.05$.

and major lipoprotein fractions also showed a general tendency of reduction with statin application and enhancement with high-cholesterol diet feeding.

The main observation can be summarized as an overall lowering of organ parasite load in all strains of mice upon diet-induced hypercholesterolemia. In LD-AE and LD-BL/6 mice, there was a significant reduction in both splenic (**Fig. 2A**, B; $P < 0.01$, $P < 0.001$) and hepatic (Fig. 2C, D; $P < 0.1$, $P < 0.0001$) parasite load in atherogenic diet fed group compared with those receiving chow

diet. LD-BALB/c mice also showed decreased splenic and hepatic parasite load in the atherogenic diet group compared with the chow diet group at three weeks postinfection ($P < 0.01$, $P < 0.05$), although no further decrease was noted at six weeks postinfection ($P < 0.0001$, $P < 0.01$) (supplementary Fig. I).

Complimentary conclusions could be drawn from the atorvastatin-treated groups. Enhanced organ parasite load was evidenced both in LD-BL/6 and LD-BABL/c upon atorvastatin treatment (Fig. 2A, C and supplementary
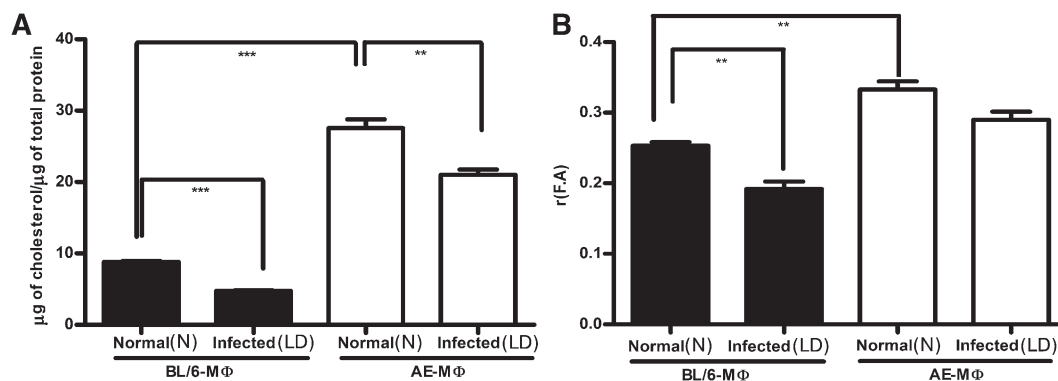

Fig. 3. Macrophage membrane cholesterol content and fluorescence anisotropy. (A) Macrophages were either kept uninfected (N) or infected (LD) with Ag83 parasites at a 1:10 ratio of cell:parasite for 48 h. Membrane was prepared from N-BL/6-Mϕ, N-AE-Mϕ, LD-BL/6-Mϕ, and LD-AE-Mϕ by ultracentrifugation. Total membrane cholesterol (free and esterified) was estimated using Amplex Red kit and expressed as micrograms of cholesterol per micrograms of total protein. (B) Fluorescence anisotropy [r(F.A.)] values under identical condition using DPH as a probe. The data represents mean ± SEM from three different experiments. ***$P < 0.001$, **$0.001 < P < 0.01$, *$0.01 < P < 0.05$.

Fig. I; $P < 0.001$, $P < 0.01$, $P < 0.05$) at three weeks postin- fection, which further increased remarkably at six weeks postinfection. In LD-AE mice, there was an initial in- crease in parasite load in both spleen and liver com- pared with chow diet animals. However, marginal rise was evident in splenic parasite load with longitudinal in- fection, whereas nonsignificant changes were observed in hepatic parasite load with time (Fig. 2B, D; $P < 0.0001$, $P < 0.05$).

Increased membrane cholesterol and higher membrane rigidity of AE macrophage compared with its wild-type counterpart

Macrophage membrane cholesterol was determined both in mutant and wild-type mice. It was observed that N-AE-Mϕ showed 3-fold higher membrane cholesterol (both free and esterified) compared with N-BL/6-Mϕ (**Fig. 3A**; $P < 0.0001$). In vitro infection given for 48 h showed equivalent parasite count in LD-BL/6-Mϕ and LD- AE-Mϕ (supplementary Fig. II). Further experiments were conducted under similar conditions. At 48 h LD infection, there was a significant decrease in membrane cholesterol both in LD-BL/6-Mϕ and LD-AE-Mϕ compared with their normal counterparts; the magnitude of decrease was greater in LD-BL/6-Mϕ than in LD-AE-Mϕ, as the latter maintained 4-fold higher membrane cholesterol than the former (Fig. 3A).

Membrane fluidity in terms of FA was determined by using DPH as a probe. There was a 40% higher FA value for N-AE-Mϕ than for N-BL/6-Mϕ, indicating an inherent rigid membrane for the former (Fig. 3B; $P < 0.01$). It was observed that there was a 30% decrease in the FA value upon LD infection at 48 h in the wild-type macrophage, whereas the same decrease for the AE macrophage was only 11%.
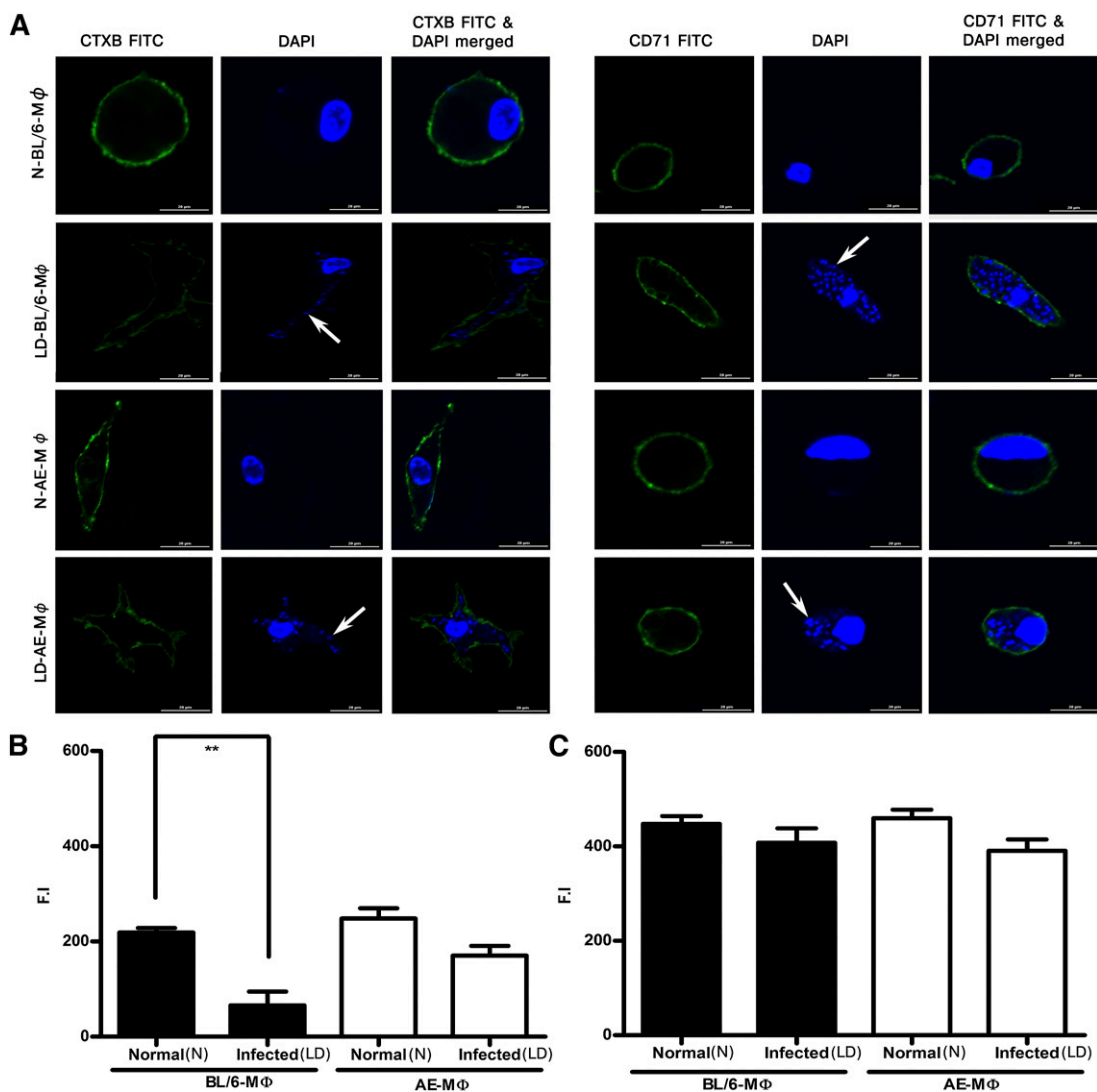

Fig. 4. Confocal studies in macrophage raft architecture. (A) Fluorescent intensities after binding of CTX-B-FITC and CD-71-FITC in N-BL/6-Mϕ, LD-BL/6-Mϕ, N-AE-Mϕ, and LD-AE-Mϕ. Cells were fixed in 1% paraformaldehyde and observed under a confocal laser scan- ning microscope. The white arrows indicate intracellular amastigotes. The resulting fluorescence intensities (F.I.) were quantified and plotted: (B) CTX-B and (C) CD71. The data represents mean ± SEM from three different experiments. ***$P < 0.001$, **$0.001 < P < 0.01$, *$0.01 < P < 0.05$.

Raft organization remained intact in LD-AE-Mφ but not in LD-BL/6-Mφ

To investigate raft and nonraft architecture, we used CTX-B-FITC, which binds to GM1 ganglioside, and transferin receptor CD71, respectively, as probes. Extent of anti-CD71 biotin binding was studied using streptavidin-FITC. Confocal images of macrophages, either normal or parasitized (**Fig. 4A**), showed that CTX-B stained N-BL/6-Mφ, N-AE-Mφ, and LD-AE-Mφ effectively but not LD-BL/6-Mφ ($P < 0.01$), whereas CD71 staining remained unaltered in all cases (Fig. 4B, C).

AE macrophages are better antigen presenters than BL/6 macrophages

The antigen-presenting ability of N-BL/6-Mφ, LD-BL/6-Mφ, N-AE-Mφ, and LD-AE-Mφ were studied based on their ability to drive anti-Ova T-cell hybridoma 13.8, in the presence or absence of ovalbumin. The T-cell stimulating ability was assayed on the basis of resulting IL-2 production. The T-cell stimulating ability was significantly higher for N-AE-Mφ compared with N-BL/6-Mφ. There was about a 50% decrease in IL-2 production when LD-BL/6-Mφ was used as APC compared with normal macrophages (**Fig. 5A**; $P < 0.01$), whereas T-cell stimulating ability in LD-AE-Mφ was marginally compromised compared with the uninfected counterpart (Fig. 5A). The efficient T-cell stimulating ability of N-AE-Mφ was not due to higher MHC class II compared with the wild-type macrophage, as essentially similar magnitudes of I-A^b

expression were observed regardless of the type of macrophage population, which was evident from anti-I-A^b-FITC staining and corresponding MFI values (Fig. 5B).

Efficient synapse formation of AE macrophage with T cells

Using intracellular Ca^{2+} mobilization in T cells as an indirect but effective functional readout, we assessed the synapse formation between T cells and macrophages. When ova-pulsed N-BL/6-Mφ was mixed with anti-ova hybridoma, there was an intracellular Ca^{2+} mobilization in T cells that was compromised when LD-BL/6-Mφ were used as APC (Fig.5C, upper panel) Interestingly, both N-AE-Mφ and LD-AE-Mφ showed T-cell stimulating ability essentially in equal measure (Fig. 5C, lower panel).

Differential modulation of cytokine repertoire in LD-AE versus wild-type mice

The splenocytes were isolated from normal, three-week-infected, and six-week-infected mice and were stimulated with 50 µg/ml SLA. The resulting cytokine production in the supernatant was studied by ELISA. The following cytokines were studied: IL10, IL-4, and TGF-β as prototypes of disease-promoting cytokines, and IL-2, IFN-γ, TNF-α, IL-12, IL-6, IL-17, and IL-22 as prototypes of host-protective cytokines (**Fig. 6**).

High levels of IL-10 and IL-4 production was monitored in both AE and BL/6 mice as early as three weeks
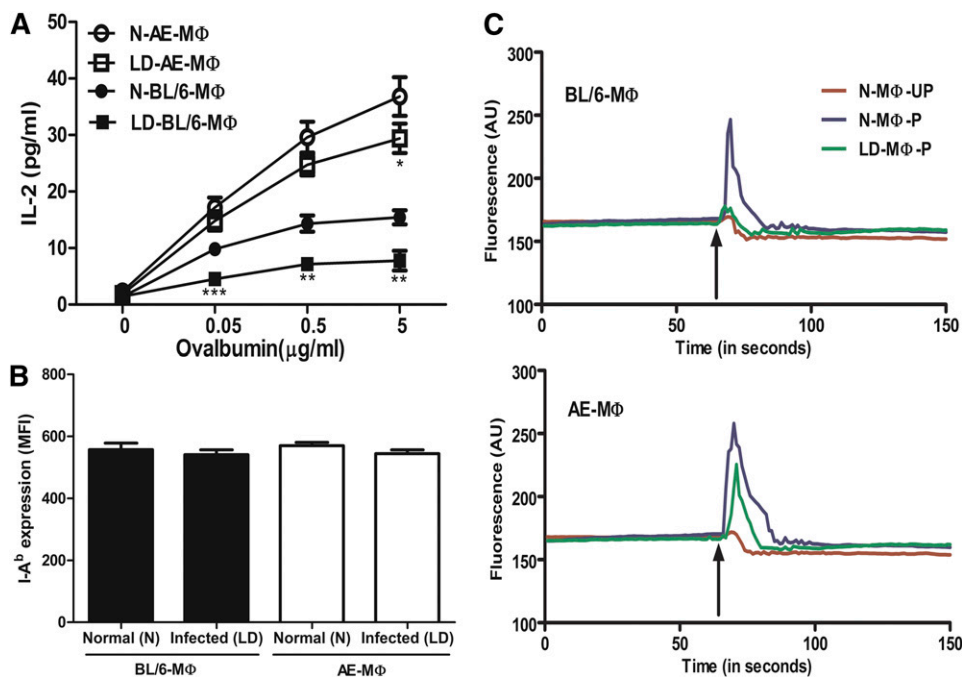

Fig. 5. T-cell (anti-Ova T-cell hybridoma 13.8) stimulating ability of N-BL/6-Mφ, LD-BL/6 -Mφ, N-AE-Mφ, and LD-AE-Mφ as a function of antigen concentration. (A) The T-cell stimulating ability was assayed in terms of IL-2 production. Data represents mean ± SEM from three different experiments. (B) Quantification of MHC molecule by FACS analysis. Cells were stained with anti-IA^b and MFI was presented. Data points are mean ± SD from triplicates. (C) Mobilization of intracellular Ca^{2+} in T cells. T cells (13.8) were loaded with fluo4-AM and then mixed with ovalbumin pulsed or unpulsed APCs. Synapse formation was assayed in terms of intracellular Ca^{2+} mobilization in T cells. The arrow indicates time of addition of APCs to the fluo4-AM-loaded T cells. BL/6 (upper panel) and AE (lower panel). P, antigen pulsed; UP, antigen unpulsed. Shown is one representative picture from three different experiments. ***$P < 0.001$, **$0.001 < P < 0.01$, *$0.01 < P < 0.05$.

postinfection. However, at six weeks postinfection, both IL-4 and IL-10 decreased significantly in LD-AE mice and increased in LD-BL/6 mice ($P < 0.0001$). Intrinsic TGF-β production was marginally lower in AE mice than in BL/6 mice; it progressively increased with longitudinal infection.

The picture was essentially opposite as far as other cytokines were concerned. In contrast to LD-BL/6 mice, IFN-γ showed a dramatic surge at three weeks postinfection, which increased further at six weeks postinfection ($P < 0.0001$) in LD-AE mice. IFN-γ:IL-10 ratio, a determinant of host protection, was higher in LD-AE mice compared with wild-type infected mice (data not shown). Significant difference in

IL-2 production between LD-AE and LD-BL/6 mice was found at six weeks postinfection. IL-12, the stimulator of Th1 subset differentiation, and TNF-α are the two most important cytokines in relation to Th1 function, and they showed a similar trend. In LD-BL/6, IL-12 showed slight increase, whereas a remarkable surge was observed in LD-AE mice ($P < 0.0001$). TNF-α was heavily enhanced in both LD-BL/6 and LD-AE mice, although the rate of increase in AE far exceeded that of BL/6 ($P < 0.0001$).

Intrinsic IL-17 production was greater in AE mice ($P < 0.05$), which increased further until six weeks postinfection ($P < 0.0001$). The pattern of IL-6 production was essentially
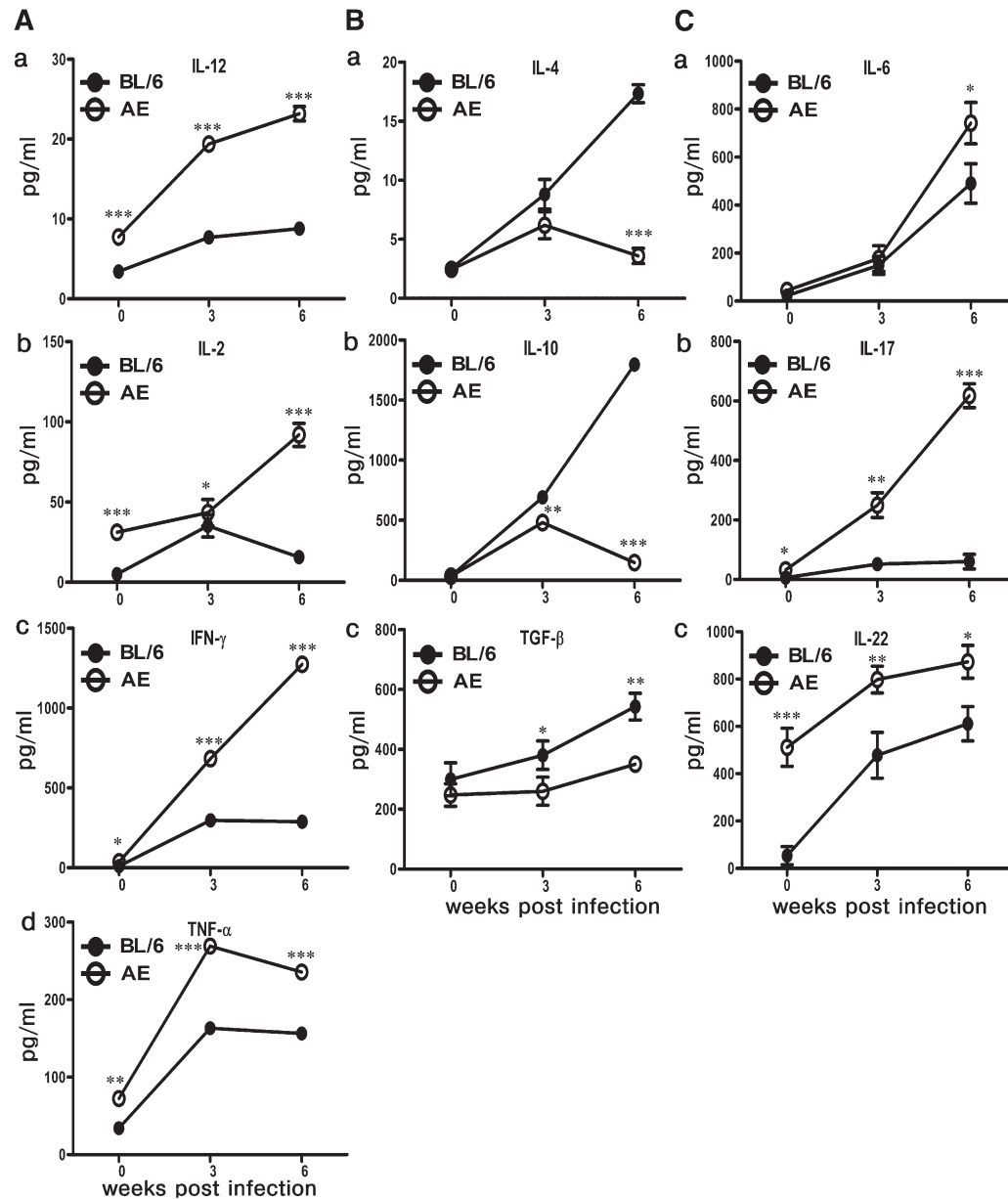

Fig. 6. Analysis of cytokine profile. Splenocytes of normal, three weeks postinfection, and six weeks postinfection BL/6 and AE animals were stimulated with 50 µg of SLA for 72 h. The resulting supernatant was collected, and cytokines were measured by ELISA. (A) Th1 type IL-12, IL-2, IFN-γ, and TNF-α. (B) Th2 type IL-4, IL-10, and TGF-β. (C) Th17 type IL-6, IL-17, and IL-22. The data represents mean ± SEM from three different experiments. ***$P < 0.001$, **$0.001 < P < 0.01$, *$0.01 < P < 0.05$.

similar in LD-AE and LD-BL/6 mice. However, at six weeks postinfection, IL-6 production was slightly higher in LD-AE mice compared with the wild-type counterpart ($P < 0.05$). Interestingly, normal AE mice intrinsically showed much higher IL-22 compared with the wild-type counterpart ($P < 0.001$). With gradual infection, IL-22 production increased in both strains, with LD-AE always showing a higher value.

Higher expansion of CD8$^+$ T cells in LD-AE mice leading to host-protective cytokine production

Frequencies of IFN-γ-producing and TNF-α-producing cells both in CD4$^+$ T cells and in the CD8$^+$ T-cell compartment were analyzed. There was no difference in IFN-γ-producing antileishmanial CD4$^+$ T cells in LD-AE and LD-BL/6 mice in a progressive infection. There was a marginal increase in the antileishmanial TNF-α-producing CD4$^+$ T cell in LD-AE at three weeks postinfection, which returned to a comparable level at six weeks postinfection. Not much difference was observed between the two strains in the CD4$^+$IFN-γ$^+$TNF-α$^+$ T-cell population between LD-AE and LD-BL/6. The picture was dramatically different in the CD8$^+$ T-cell compartment. There was a significant increase in the frequencies of IFN-γ-producing CD8$^+$ T cells in LD-AE mice ($P < 0.01$, $P < 0.05$) in a progressive infection (almost 3- to 4-fold higher expression) compared with wild-type. CD8$^+$TNF-α$^+$ T-cell population was almost similar in LD-AE and LD-BL/6. However, the CD8$^+$IFN-γ$^+$TNF-α$^+$ T-cell population increased around 5 times in LD-AE mice ($P < 0.01$, $P < 0.05$), whereas in LD-BL/6, such expansion was not observed (**Fig. 7** and supplementary Fig. III).

Transcription factors to drive Th1, Th2, and Th17 were differentially expressed in normal, LD-BL/6, and LD-AE mice

Status of T-bet, GATA3, and ROR-γt, the prerequisite transcription factors to drive Th1, Th2, and Th17 development,

respectively, was studied in normal animals and in LD-BL/6 and LD-AE mice. Total RNA was prepared from the splenocytes of normal, three-week-infected, and six-week-infected mice, and real time RT-PCR was performed for the mRNA levels.

We observed that there was a marginal increase in T-bet expression in splenocytes at three weeks postinfection compared with normal in both strains. At six weeks postinfection, the T-bet expression in LD-BL/6 did not differ much, whereas a significant increase was seen in LD-AE (**Fig. 8B**). The expression of GATA3 increased about 3-fold at three weeks postinfection and about 15-fold at six weeks postinfection in LD-BL/6 mice. However, the picture of GATA3 in LD-AE mice is different. At three weeks postinfection, there was about 2-fold increase, but it decreased thereafter at six weeks postinfection (Fig.8C). The status of ROR-γt expression in normal AE mice was higher than in normal BL/6 mice. Expression of ROR-γt remained more or less unaltered at three weeks postinfection and decreased at six weeks postinfection in LD-BL/6 mice. On the other hand, its expression increased gradually in LD-AE mice with progressive infection (Fig. 8A).

Hepatic granuloma is formed preferentially in LD-AE mice

To understand the tissue response in LD infection, we performed hematoxylin and eosin staining in liver sections of both LD-BL/6 and LD-AE mice at six weeks postinfection. Photomicrographs from different microscopic fields in LD-BL/6 mice showed partial loss in tissue architecture with no detectable granuloma formation, Kupffer cell hyperplasia, or mixed inflammatory cell infiltration and scant LD bodies (**Fig. 9A**). In contrast, photomicrographs from LD-AE mice revealed zones of well-formed, mature and immature granuloma, Kupffer cells with zonal infiltration of lymphocytes in periportal area, sinusoidal dilation,
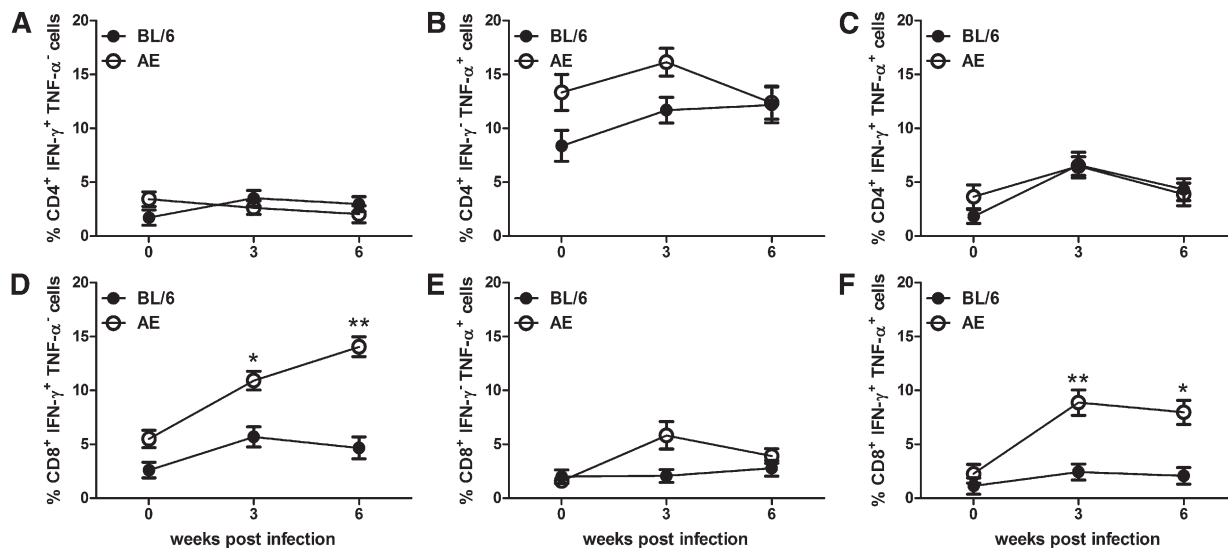

Fig. 7. Percentage of IFN-γ and TNF-α producing T-cell population in CD4$^+$ and CD8$^+$ T-cell counterparts in the splenocytes of infected mice. Splenocytes were stimulated as described in Fig. 6. (A) Percentage of CD4$^+$IFN-γ$^+$TNF-α$^-$ T cell. (B) Percentage of CD4$^+$IFN-γ$^-$TNF-α$^+$ T cell. (C) Percentage of CD4$^+$IFN-γ$^+$TNF-α$^+$ T cell. (D) Percentage of CD8$^+$IFN-γ$^+$TNF-α$^-$ T cell.(E) Percentage of CD8$^+$IFN-γ$^-$TNF-α$^+$ T cell (F) Percentage of CD8$^+$IFN-γ$^+$TNF-α$^+$ T cell. The data represents mean ± SEM from three different experiments. ***$P < 0.001$, **$0.001 < P < 0.01$, *$0.01 < P < 0.05$.
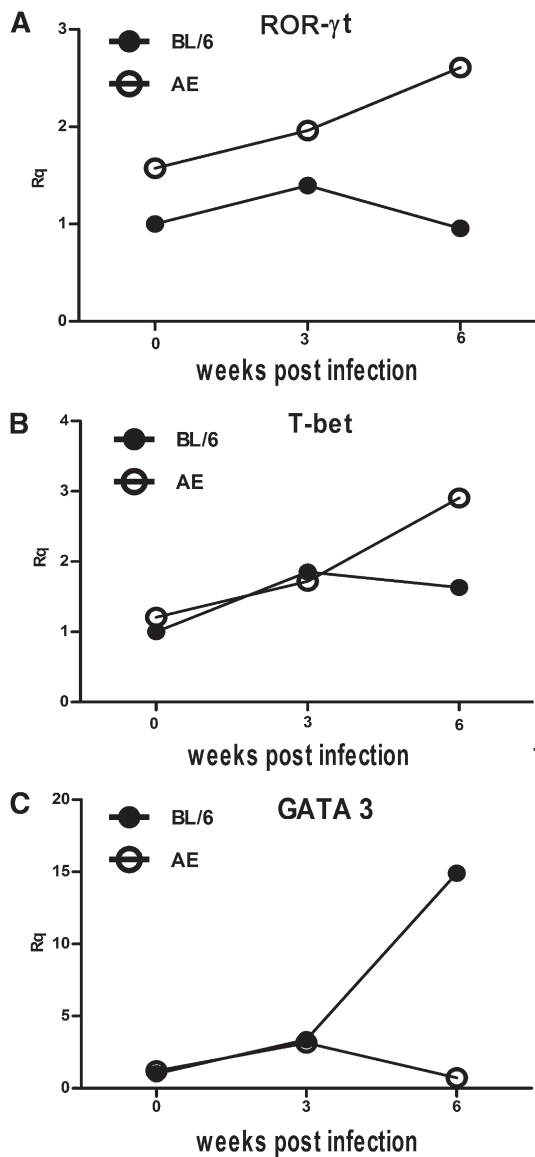
Fig. 8. Expression of transcription factor. Splenocytes were isolated from normal, three weeks postinfection, and six weeks postinfection BL/6 and AE animals, and total RNA was prepared. Quantitative RT-PCR was performed and signals were normalized against β-Actin. (A) ROR-γt. (B) T-bet. (C) GATA3. Data points are relative fold changes (R_q) with respect to normal BL/6 values. Basically, $2^{-\Delta Ct}$ [where ΔCt = Threshold cycle (Ct) target − Threshold cycle of endogenous control (here, β-actin)] values were calculated for each group from three different experiments. Means were determined and represented as fold changes taking normal BL/6 to be one.

engorged blood vessels, mild periportal fibrosis, focal collection of neutrophilic infiltration, and fatty changes in hepatocytes (Fig. 9B).

DISCUSSION

Hypocholesterolemia is largely evidenced in visceral leishmaniasis (8, 9). Previous study from our group showed that there is a significant decrease in membrane cholesterol in LD-infected macrophages (46) and that liposomal delivery of cholesterol in LD-infected hamsters therapeutically

offers strong protection (7). In the present study, we reevaluated the protective role of cholesterol in VL. We used two strains of mice congenic with respect to apoE gene products. A deletion mutation in *apoe* causes defective cholesterol metabolism, leading to hypercholesterolemia (23).

The primary observation is the resistance of AE mice to LD infection. Further manipulation of serum cholesterol by exogenous means in both wild-type and AE animals showed that cholesterol content has a direct bearing on VL pathogenesis. Diet-induced hypercholesterolemia in BL/6 mice renders them resistant to LD infection. A similar finding was observed in BALB/c mice, a model particularly known to be susceptible to LD infection. Hence, modulating the cholesterol content in any normal mice can make them behave like AE mice, as far as *Leishmania donovani* infection is concerned. Reversibly, hypocholesterolemia induced by statin treatment can lead to further susceptibility not only in BL/6 and BALB/c mice but also in AE mice. It is important to note that statin-treated AE mice did not show an increased parasitemia at six weeks postinfection; rather, a slight drop was evident in liver parasite load. This observation can be attributed to the intrinsic tendency to maintain high cholesterol even under statin treatment and thus control further parasite growth. Hence, from all these models, it can be inferred that it is hypercholesterolemia and not the deficiency of apoE that rules the LD infection propagation in murine hosts.

In vitro infection showed comparable intracellular parasites in macrophages derived from both BL/6 and AE mice. Interestingly, LD-AE-Mφ, like N-AE-Mφ and N-BL/6-Mφ, showed essentially normal raft architecture and efficient T-cell activation; these abilities were compromised in LD-BL/6-Mφ, which may contribute to defective immune response in LD-BL/6 mice. It is worth mentioning that N-AE-Mφ was a much better antigen presenter than N-BL/6-Mφ. This difference was not due to the MHC II (I-A[b]) molecule as evident from its similar expression on the cell surface. From all these findings, it can be concluded that, even under similar infection, LD-AE-Mφ shows proper macrophage function and is successful in mounting an effective immune response that finally helps in the protection associated with AE mice. It can also be concluded that apoE is not directly related to LD-macrophage interaction, as that would have resulted in differential parasite count in infected macrophages derived from BL/6 and AE mice.

Cholesterol is a critical determinant for the maintenance of lipid rafts (47). Defined rafts may increase the number of peptide-MHC complexes, and disruption of lipids rafts by methyl β-cyclodextrin treatment impairs the presentation of peptides to MHC complexes (48). The N-AE-Mφ showed essentially 3-fold higher membrane cholesterol compared with N-BL/6-Mφ, which was reflected in the FA value. In contrast to LD-BL/6-Mφ, LD-AE-Mφ showed no significant change in membrane cholesterol. A similar finding is reported in leprosy where increased membrane fluidity coupled with raft disruption proved a major reason for defective antigen presentation (49).
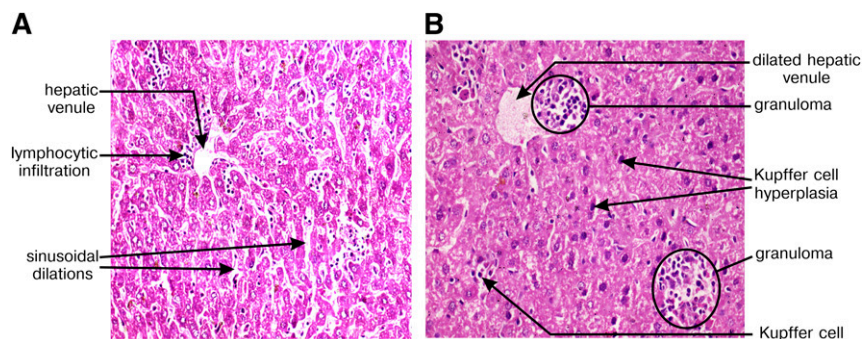
Fig. 9. Hepatic cellular response to *L. donovani* infection. Hematoxylin and eosin staining was performed from liver tissue samples. Photomicrographs of mice liver section six weeks postinfection in (A) BL/6 and (B) AE mice. Different features are highlighted in the photomicrograph. Magnification is ×400.

The above observations indicate that otherwise normal APC function of LD-AE-Mφ may favor the expansion of antileishmanial T-cell repertoire in LD-AE. It was observed that in LD-AE mice there is an expansion of antileishmanial CD8$^+$IFN-γ$^+$ and CD8$^+$IFN-γ$^+$TNF-α$^+$ T cells. Previous report shows *L. donovani* parasites evade CD8$^+$ T-cell responses by limiting their expansion (50). However, the importance of CD8$^+$ T cells in antileishmanial defense is well documented in vaccination studies (51). To our knowledge, this is the first report of detectable expansion of antileishmanial CD8$^+$ T cells in experimental infection. Cholesterol influences cross presentation and enhances the activation of CD8$^+$ T cells to exogenous antigen (52). It is tempting to speculate that similar phenomena may be operative in LD-AE mice due to endogenous hypercholesterolemia.

To explore further the T-cell repertoire in infection, the status of the transcriptions factors that govern Th1, Th2, and Th17 cell development were evaluated. Involvement of T-bet and GATA3 in development of Th1 and Th2 subset, respectively, is well established (53, 54). An increased T-bet expression in LD-AE mice may well explain the surge of IFN-γ at six weeks postinfection. A lower T-bet expression along with an increased GATA3 expression is well supported by a higher IL-4 level in LD-BL/6 mice. Quite convincingly, IL-10, well associated with the disease progression (55–57), was found in a much higher level in LD-BL/6 compared with LD-AE. Development and differentiation of the Th17 subset is controlled by the transcription factor ROR-γt (58), and IL-17 and IL-22 are known to be associated with protection against kala-azar (59). Here we found that ROR-γt is expressed to a greater extent in LD-AE mice. In agreement, the IL-17 family of cytokines, such as IL-6, IL-17, and IL-22, increases dramatically at six weeks postinfection in LD-AE mice as opposed to LD-BL/6 mice. Other host-protective cytokines, such as TNF-α, IL-12, and IL-2, the prototypes of Th1, are found to be enhanced in LD-AE mice, which corroborated well with the reduction in parasite load. TGF-β was always found to be enhanced in LD-BL/6, which is in accordance with the role of TGF-β in suppressing the production of IFN-γ (60). Overall, the whole cytokine milieu with predominantly host-protective ones is in favor of pathogen clearance from LD-AE mice.

Granuloma formation, a tissue response against pathogens, is influenced by IFN-γ and TNF-α (61). Interestingly, LD-AE mice but not LD-BL/6 mice developed well-formed mature hepatic granuloma.

Atherogenic diet feeding or atorvastatin treatment changed the whole lipid profile; i.e., particular alterations were observed in triglyceride and lipoprotein fractions. It is worth mentioning that other aspects of lipoprotein structure or metabolism or level of triglyceride may have some role in the observed protection associated with LD infection. These other attributes may work in synergy with cholesterol in modulating the membrane property leading to the altered LD pathogenesis.

Overall, this study shows direct evidence that hypercholesterolemia-associated changes in the lipid profile is involved with protection against visceral leishmaniasis. This may be another area of research to study the disease process and designing therapeutics by modulating host cell membrane fluidity. Therefore, it will be interesting to study the cholesterol status as a predictive marker in asymptomatic (positive for k39 but no clinical disease) individuals in kala-azar-affected areas.∎

REFERENCES

1. Kaye, P. M., M. Svensson, M. Ato, A. Maroof, R. Polley, S. Stager, S. Zubairi, and C. R. Engwerda. 2004. The immunopathology of experimental visceral leishmaniasis. *Immunol. Rev.* **201:** 239–253.
2. Kaye, P., and P. Scott. 2011. Leishmaniasis: complexity at the host-pathogen interface. *Nat. Rev. Microbiol.* **9:** 604–615.
3. Tripathi, P., V. Singh, and S. Naik. 2007. Immune response to leishmania: paradox rather than paradigm. *FEMS Immunol. Med. Microbiol.* **51:** 229–242.
4. Engwerda, C. R., M. Ato, and P. M. Kaye. 2004. Macrophages, pathology and parasite persistence in experimental visceral leishmaniasis. *Trends Parasitol.* **20:** 524–530.
5. Desjardins, M., and A. Descoteaux. 1998. Survival strategies of Leishmania donovani in mammalian host macrophages. *Res. Immunol.* **149:** 689–692.
6. Chakraborty, D., S. Banerjee, A. Sen, K. K. Banerjee, P. Das, and S. Roy. 2005. Leishmania donovani affects antigen presentation of macrophage by disrupting lipid rafts. *J. Immunol.* **175:** 3214–3224.

7. Banerjee, S., J. Ghosh, S. Sen, R. Guha, R. Dhar, M. Ghosh, S. Datta, B. Raychaudhury, K. Naskar, A. K. Haldar, et al. 2009. Designing therapies against experimental visceral leishmaniasis by modulating the membrane fluidity of antigen-presenting cells. *Infect. Immun.* **77:** 2330–2342.

8. Lal, C. S., N. Verma, V. N. Rabidas, A. Ranjan, K. Pandey, R. B. Verma, D. Singh, S. Kumar, and P. Das. 2010. Total serum cholesterol determination can provide understanding of parasite burden in patients with visceral leishmaniasis infection. *Clin. Chim. Acta.* **411:** 2112–2113.

9. Ghosh, J., C. S. Lal, K. Pandey, V. N. Das, P. Das, K. Roychoudhury, and S. Roy. 2011. Human visceral leishmaniasis: decrease in serum cholesterol as a function of splenic parasite load. *Ann. Trop. Med. Parasitol.* **105:** 267–271.

10. Muldoon, M. F., A. Marsland, J. D. Flory, B. S. Rabin, T. L. Whiteside, and S. B. Manuck. 1997. Immune system differences in men with hypo- or hypercholesterolemia. *Clin. Immunol. Immunopathol.* **84:** 145–149.

11. Jacobs, D., H. Blackburn, M. Higgins, D. Reed, H. Iso, G. McMillan, J. Neaton, J. Nelson, J. Potter, B. Rifkind, et al. 1992. Report of the Conference on Low Blood Cholesterol: mortality associations. *Circulation.* **86:** 1046–1060.

12. Miner, M. D., J. C. Chang, A. K. Pandey, C. M. Sassetti, and D. R. Sherman. 2009. Role of cholesterol in Mycobacterium tuberculosis infection. *Indian J. Exp. Biol.* **47:** 407–411.

13. Elias, E. R., M. B. Irons, A. D. Hurley, G. S. Tint, and G. Salen. 1997. Clinical effects of cholesterol supplementation in six patients with the Smith-Lemli-Opitz syndrome (SLOS). *Am. J. Med. Genet.* **68:** 305–310.

14. Sen, E., S. Chattopadhyay, S. Bandopadhyay, T. De, and S. Roy. 2001. Macrophage heterogeneity, antigen presentation, and membrane fluidity: implications in visceral Leishmaniasis. *Scand. J. Immunol.* **53:** 111–120.

15. Crane, J. M., and L. K. Tamm. 2004. Role of cholesterol in the formation and nature of lipid rafts in planar and spherical model membranes. *Biophys. J.* **86:** 2965–2979.

16. Radhakrishnan, A., T. G. Anderson, and H. M. McConnell. 2000. Condensed complexes, rafts, and the chemical activity of cholesterol in membranes. *Proc. Natl. Acad. Sci. USA.* **97:** 12422–12427.

17. Rosenberger, C. M., J. H. Brumell, and B. B. Finlay. 2000. Microbial pathogenesis: lipid rafts as pathogen portals. *Curr. Biol.* **10:** R823–R825.

18. Hartlova, A., L. Cerveny, M. Hubalek, Z. Krocova, and J. Stulik. 2010. Membrane rafts: a potential gateway for bacterial entry into host cells. *Microbiol. Immunol.* **54:** 237–245.

19. Vieira, F. S., G. Correa, M. Einicker-Lamas, and R. Coutinho-Silva. 2010. Host-cell lipid rafts: a safe door for micro-organisms? *Biol. Cell.* **102:** 391–407.

20. Gatfield, J., and J. Pieters. 2000. Essential role for cholesterol in entry of mycobacteria into macrophages. *Science.* **288:** 1647–1650.

21. Pucadyil, T. J., P. Tewary, R. Madhubala, and A. Chattopadhyay. 2004. Cholesterol is required for Leishmania donovani infection: implications in leishmaniasis. *Mol. Biochem. Parasitol.* **133:** 145–152.

22. Wunder, C., Y. Churin, F. Winau, D. Warnecke, M. Vieth, B. Lindner, U. Zahringer, H. J. Mollenkopf, E. Heinz, and T. F. Meyer. 2006. Cholesterol glucosylation promotes immune evasion by Helicobacter pylori. *Nat. Med.* **12:** 1030–1038.

23. Kypreos, K. E., and V. I. Zannis. 2006. LDL receptor deficiency or apoE mutations prevent remnant clearance and induce hypertriglyceridemia in mice. *J. Lipid Res.* **47:** 521–529.

24. Mahley, R. W. 1983. Apolipoprotein E and cholesterol metabolism. *Klin. Wochenschr.* **61:** 225–232.

25. Bu, G. 2009. Apolipoprotein E and its receptors in Alzheimer's disease: pathways, pathogenesis and therapy. *Nat. Rev. Neurosci.* **10:** 333–344.

26. de Bont, N., M. G. Netea, P. N. Demacker, B. J. Kullberg, J. W. van der Meer, and A. F. Stalenhoef. 2000. Apolipoprotein E-deficient mice have an impaired immune response to Klebsiella pneumoniae. *Eur. J. Clin. Invest.* **30:** 818–822.

27. Roselaar, S. E., and A. Daugherty. 1998. Apolipoprotein E-deficient mice have impaired innate immune responses to Listeria monocytogenes in vivo. *J. Lipid Res.* **39:** 1740–1743.

28. Martens, G. W., M. C. Arikan, J. Lee, F. Ren, T. Vallerskog, and H. Kornfeld. 2008. Hypercholesterolemia impairs immunity to tuberculosis. *Infect. Immun.* **76:** 3464–3472.

29. Price, D. A., M. F. Bassendine, S. M. Norris, C. Golding, G. L. Toms, M. L. Schmid, C. M. Morris, A. D. Burt, and P. T. Donaldson. 2006. Apolipoprotein epsilon3 allele is associated with persistent hepatitis C virus infection. *Gut.* **55:** 715–718.

30. Mukherjee, P., A. Dani, S. Bhatia, N. Singh, A. Y. Rudensky, A. George, V. Bal, S. Mayor, and S. Rath. 2001. Efficient presentation of both cytosolic and endogenous transmembrane protein antigens on MHC class II is dependent on cytoplasmic proteolysis. *J. Immunol.* **167:** 2632–2641.

31. Nachtigal, P., N. Pospisilova, G. Jamborova, K. Pospechova, D. Solichova, C. Andrys, P. Zdansky, S. Micuda, and V. Semecky. 2008. Atorvastatin has hypolipidemic and anti-inflammatory effects in apoE/LDL receptor-double-knockout mice. *Life Sci.* **82:** 708–717.

32. Mukhopadhyay, S., P. Sen, S. Bhattacharyya, S. Majumdar, and S. Roy. 1999. Immunoprophylaxis and immunotherapy against experimental visceral leishmaniasis. *Vaccine.* **17:** 291–300.

33. Saha, B., H. Nanda-Roy, A. Pakrashi, R. N. Chakrabarti, and S. Roy. 1991. Immunobiological studies on experimental visceral leishmaniasis. I. Changes in lymphoid organs and their possible role in pathogenesis. *Eur. J. Immunol.* **21:** 577–581.

34. Ferrua, B., Y. Le Fichoux, I. Suffia, D. Rousseau, C. Roptin, and J. Kubar. 2001. Quantitation of Leishmania infantum in tissues of infected BALB/c mouse by sandwich ELISA. *J. Immunoassay Immunochem.* **22:** 165–181.

35. McElrath, M. J., H. W. Murray, and Z. A. Cohn. 1988. The dynamics of granuloma formation in experimental visceral leishmaniasis. *J. Exp. Med.* **167:** 1927–1937.

36. Goto, Y., L. Y. Bogatzki, S. Bertholet, R. N. Coler, and S. G. Reed. 2007. Protective immunization against visceral leishmaniasis using Leishmania sterol 24-c-methyltransferase formulated in adjuvant. *Vaccine.* **25:** 7450–7458.

37. Saha, S., S. Mondal, R. Ravindran, S. Bhowmick, D. Modak, S. Mallick, M. Rahman, S. Kar, R. Goswami, S. K. Guha, et al. 2007. IL-10- and TGF-beta-mediated susceptibility in kala-azar and post-kala-azar dermal leishmaniasis: the significance of amphotericin B in the control of Leishmania donovani infection in India. *J. Immunol.* **179:** 5592–5603.

38. Pala, P., T. Hussell, and P. J. Openshaw. 2000. Flow cytometric measurement of intracellular cytokines. *J. Immunol. Methods.* **243:** 107–124.

39. Bhaumik, S. K., K. Naskar, and T. De. 2009. Complete protection against experimental visceral leishmaniasis with complete soluble antigen from attenuated Leishmania donovani promastigotes involves Th1-immunity and down-regulation of IL-10. *Eur. J. Immunol.* **39:** 2146–2160.

40. Titus, R. G., A. Kelso, and J. A. Louis. 1984. Intracellular destruction of Leishmania tropica by macrophages activated with macrophage activating factor/interferon. *Clin. Exp. Immunol.* **55:** 157–165.

41. Pucadyil, T. J., and A. Chattopadhyay. 2004. Exploring detergent insolubility in bovine hippocampal membranes: a critical assessment of the requirement for cholesterol. *Biochim. Biophys. Acta.* **1661:** 9–17.

42. Amundson, D. M., and M. Zhou. 1999. Fluorometric method for the enzymatic determination of cholesterol. *J. Biochem. Biophys. Methods.* **38:** 43–52.

43. Shinitzky, M., and M. Inbar. 1974. Difference in microviscosity induced by different cholesterol levels in the surface membrane lipid layer of normal lymphocytes and malignant lymphoma cells. *J. Mol. Biol.* **85:** 603–615.

44. Shinitzky, M., and Y. Barenholz. 1978. Fluidity parameters of lipid regions determined by fluorescence polarization. *Biochim. Biophys. Acta.* **515:** 367–394.

45. Jambrina, E., R. Alonso, M. Alcalde, M. del Carmen Rodriguez, A. Serrano, A. C. Martinez, J. Garcia-Sancho, and M. Izquierdo. 2003. Calcium influx through receptor-operated channel induces mitochondria-triggered paraptotic cell death. *J. Biol. Chem.* **278:** 14134–14145.

46. Sen, S., K. Roy, S. Mukherjee, R. Mukhopadhyay, and S. Roy. 2011. Restoration of IFNgammaR subunit assembly, IFNgamma signaling and parasite clearance in Leishmania donovani infected macrophages: role of membrane cholesterol. *PLoS Pathog.* **7:** e1002229.

47. Simons, K., and W. L. Vaz. 2004. Model systems, lipid rafts, and cell membranes. *Annu. Rev. Biophys. Biomol. Struct.* **33:** 269–295.

48. Anderson, H. A., E. M. Hiltbold, and P. A. Roche. 2000. Concentration of MHC class II molecules in lipid rafts facilitates antigen presentation. *Nat. Immunol.* **1:** 156–162.

49. Kumar, S., R. A. Naqvi, N. Khanna, and D. N. Rao. 2011. Disruption of HLA-DR raft, deregulations of Lck-ZAP-70-Cbl-b cross-talk

and miR181a towards T cell hyporesponsiveness in leprosy. *Mol. Immunol.* **48:** 1178–1190.

50. Joshi, T., S. Rodriguez, V. Perovic, I. A. Cockburn, and S. Stager. 2009. B7-H1 blockade increases survival of dysfunctional CD8(+) T cells and confers protection against Leishmania donovani infections. *PLoS Pathog.* **5:** e1000431.

51. Mazumder, S., M. Maji, and N. Ali. 2011. Potentiating effects of MPL on DSPC bearing cationic liposomes promote recombinant GP63 vaccine efficacy: high immunogenicity and protection. *PLoS Negl. Trop. Dis.* **5:** e1429.

52. Albrecht, I., J. Gatfield, T. Mini, P. Jeno, and J. Pieters. 2006. Essential role for cholesterol in the delivery of exogenous antigens to the MHC class I-presentation pathway. *Int. Immunol.* **18:** 755–765.

53. Rao, A., and O. Avni. 2000. Molecular aspects of T-cell differentiation. *Br. Med. Bull.* **56:** 969–984.

54. Bowen, H., A. Kelly, T. Lee, and P. Lavender. 2008. Control of cytokine gene transcription in Th1 and Th2 cells. *Clin. Exp. Allergy.* **38:** 1422–1431.

55. Wilson, M. E., S. M. Jeronimo, and R. D. Pearson. 2005. Immunopathogenesis of infection with the visceralizing Leishmania species. *Microb. Pathog.* **38:** 147–160.

56. Stanley, A. C., and C. R. Engwerda. 2007. Balancing immunity and pathology in visceral leishmaniasis. *Immunol. Cell Biol.* **85:** 138–147.

57. Nylén, S., and D. Sacks. 2007. Interleukin-10 and the pathogenesis of human visceral leishmaniasis. *Trends Immunol.* **28:** 378–384.

58. Ivanov, I. I., B. S. McKenzie, L. Zhou, C. E. Tadokoro, A. Lepelley, J. J. Lafaille, D. J. Cua, and D. R. Littman. 2006. The orphan nuclear receptor RORgammat directs the differentiation program of proinflammatory IL-17+ T helper cells. *Cell.* **126:** 1121–1133.

59. Pitta, M. G., A. Romano, S. Cabantous, S. Henri, A. Hammad, B. Kouriba, L. Argiro, M. el Kheir, B. Bucheton, C. Mary, et al. 2009. IL-17 and IL-22 are associated with protection against human kala azar caused by Leishmania donovani. *J. Clin. Invest.* **119:** 2379–2387.

60. Wilson, M. E., B. M. Young, B. L. Davidson, K. A. Mente, and S. E. McGowan. 1998. The importance of TGF-beta in murine visceral leishmaniasis. *J. Immunol.* **161:** 6148–6155.

61. Murray, H. W. 2001. Tissue granuloma structure-function in experimental visceral leishmaniasis. *Int. J. Exp. Pathol.* **82:** 249–267.